RESEARCH ARTICLE

Enhanced Photocatalytic Degradation of Organic Pollutants Using Iron Lanthanum Oxide Nanoparticles

Sajid Ali Ansari[1],*, Nazish Parveen[2]

ABSTRACT: This study investigates the synthesis, characterization, and photocatalytic performance of iron lanthanum oxide nanoparticles (FeLO NPs) tailored for environmental remediation applications. The nanoparticles were synthesized using a co-precipitation method involving ferrous and lanthanum nitrates, followed by pH adjustment and calcination. Characterization techniques including X-ray diffraction (XRD), scanning electron microscopy (SEM), and Fourier-transform infrared spectroscopy (FTIR) were employed to analyze the structural and morphological properties of the nanoparticles. XRD confirmed the crystalline nature of FeLO NPs with peaks corresponding to standard indices, while SEM images revealed a heterogeneous surface topology conducive to catalytic activity. FTIR analysis detected functional groups and bonding interactions indicative of the complex molecular composition of the nanoparticles. The Brunauer-Emmett-Teller (BET) method determined a surface area of 2.43 m²/g. Photocatalytic testing using methylene blue (MB) under UV and visible light showed that FeLO NPs achieved up to 90% degradation of the dye, highlighting their effectiveness in pollutant breakdown. The degradation mechanism involved the formation of electron-hole pairs, facilitating radical generation and subsequent pollutant decomposition. This study underscores the potential of FeLO NPs as efficient and sustainable photocatalysts for the treatment of dye-polluted wastewater.

Keywords: FeLO Nanoparticles; Photocatalysis; Water Remediation; Organic Pollutants; Surface Analysis

1. INTRODUCTION

Ferric lithium oxide ($FeLiO_3$) nanoparticles exhibit promising applications as photocatalysts in environmental remediation, particularly in the degradation of organic pollutants under UV light [1-5]. These nanoparticles leverage their unique electronic properties to harness UV radiation effectively, initiating a photocatalytic reaction that decomposes complex pollutants into less harmful substances. The process begins when UV light interacts with $FeLiO_3$, causing electrons in the valence band to become excited and jump to the conduction band, thus generating electron-hole pairs. These electron-hole pairs are crucial in the photocatalytic process. The electrons in the conduction band can react with dissolved oxygen in the water to form superoxide radicals ($•O^{2-}$), while the holes in the valence band can generate hydroxyl radicals ($•OH$) by reacting with water molecules or hydroxide ions [3-7]. These radicals are highly reactive and play a vital role in breaking down organic pollutants into smaller, non-toxic molecules such as carbon dioxide and water.

The effectiveness of $FeLiO_3$ nanoparticles in photocatalysis is significantly enhanced by their ability to facilitate the rapid separation and migration of photogenerated charge carriers, minimizing recombination and maximizing radical formation [8-10]. This enhanced charge separation contributes to the high degradation rates observed in pollutants. Additionally, the stability and reusability of $FeLiO_3$ make it a sustainable choice for continuous use in water treatment systems, offering a practical solution for the purification of polluted water bodies

[1] Department of Physics, College of Science, King Faisal University, King Faisal University, P. O. Box 400, Hafouf, Al-Ahsa 31982, Kingdom of Saudi Arabia

[2] Department of Chemistry, College of Science, King Faisal University, King Faisal University, P. O. Box 400, Hafouf, Al-Ahsa 31982, Kingdom of Saudi Arabia

*Author to whom correspondence should be addressed:
sansari@kfu.edu.sa (S. A. Ansari)

[11-16]. Thus, $FeLiO_3$ nanoparticles stand out as efficient and durable photocatalysts in the field of environmental cleanup.

This research explores the development, analysis, and photocatalytic efficacy of iron lanthanum oxide nanoparticles (FeLO NPs), designed specifically for cleaning up environmental contaminants. These nanoparticles were produced through a co-precipitation technique using solutions of iron and lanthanum nitrates, followed by a careful adjustment of pH and a calcination process. A range of characterization methods, such as X-ray diffraction (XRD), scanning electron microscopy (SEM), and Fourier-transform infrared spectroscopy (FTIR), were utilized to evaluate the structural and surface attributes of the nanoparticles. The XRD results verified the crystalline structure of the FeLO NPs, with peaks aligning with known indices. SEM provided insights into the irregular surface morphology that enhances their catalytic effectiveness. FTIR measurements identified various functional groups and bonds, reflecting the nanoparticles' intricate chemical structure. Surface area measurements conducted via the Brunauer-Emmett-Teller (BET) technique showed a value of 2.43 m²/g. In photocatalytic tests, these nanoparticles successfully decomposed up to 90% of methylene blue under both UV and visible light, demonstrating their potential for degrading similar pollutants. The process involved generating electron-hole pairs that facilitated the formation of radicals needed for breaking down the contaminants, highlighting the capabilities of FeLO NPs in treating wastewater contaminated with dyes.

2. EXPERIMENTAL DETAILS

2.1. Materials and Methods

The structural properties of the FeLO nanoparticles were analyzed using several techniques. X-ray diffraction measurements were carried out with an Analytica PW1830 instrument, while Fourier-transform infrared spectroscopy (FTIR) was conducted using a PerkinElmer BX-spectrum device. The specific surface area of the FeLO nanoparticles was assessed using a Nova 2200e QuantaChrome BET surface area analyzer. Additionally, the external and internal morphology of the nanoparticles was examined using a Zeiss SIGMA VP scanning electron microscope, based in Germany.

2.2 Synthesis of FeLO NPs

Iron lanthanum oxide nanoparticles (FeLO NPs) were fabricated using a co-precipitation approach. Solutions of 0.1M ferrous nitrate and lanthanum nitrate were independently prepared in deionized water. These solutions were then combined and subjected to stirring with a magnetic stirrer at 60 °C for 30 minutes. To adjust the pH to 9, ammonium hydroxide was incrementally added to the mixture while it was continuously heated and stirred. Following an hour of this process, a precipitate formed which was subsequently rinsed with water and dried at 80 °C. To complete the synthesis, the dried precipitate was calcined at 500 °C for four hours (Figure 1).

3. RESULTS AND DISCUSSION

X-ray diffraction (XRD) analysis was utilized to determine the crystalline structure of the FeLO nanoparticles (Figure 2). The XRD patterns revealed that the nanoparticles are crystalline, with distinct peaks observed at specific 2θ° angles. These peaks, occurring at 22.64 (110), 25.90 (111), 32.29 (121), 39.8 (220), 46.33 (202), 57.48 (240), and 67 (242), correspond closely to the standard JCPDS file number 37-1493 [4-8]. This confirmation of peak positions indicates a well-defined crystalline phase within the synthesized nanoparticles, displaying their structured atomic arrangement.

Scanning electron microscopy was employed to examine the surface morphology of the FeLO nanoparticles, as depicted in the accompanying figure. The analysis revealed that the nanoparticles were distributed in an irregular pattern (Figure 3). This arrangement suggests a varied surface topology across the sample. Furthermore, the heterogeneity observed on the surfaces of these nanoparticles indicates a complex and uneven textural characteristic. This structural diversity can potentially influence the reactive properties of the nanoparticles, making them suitable for various applications where surface interactions are crucial.
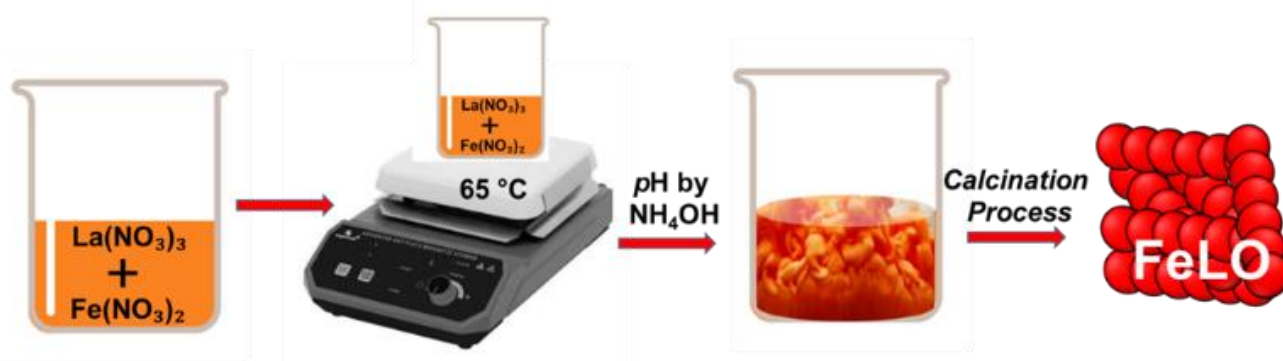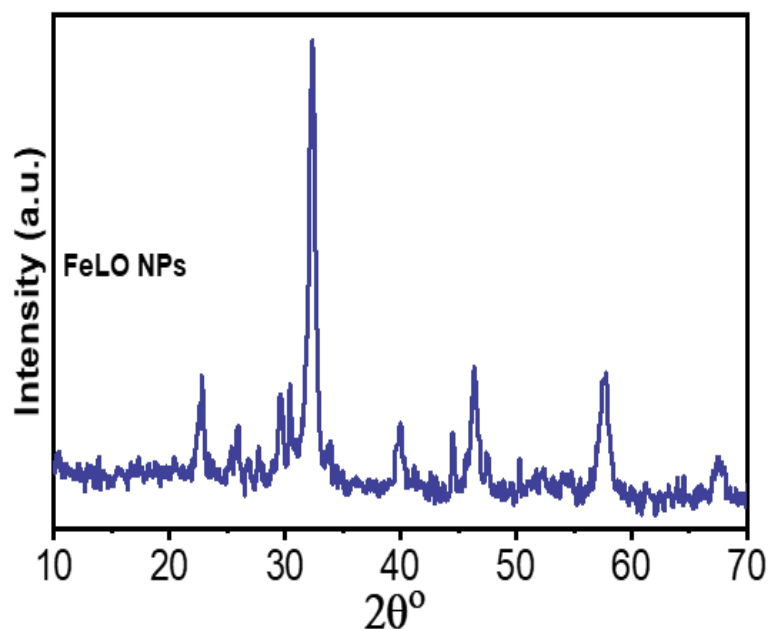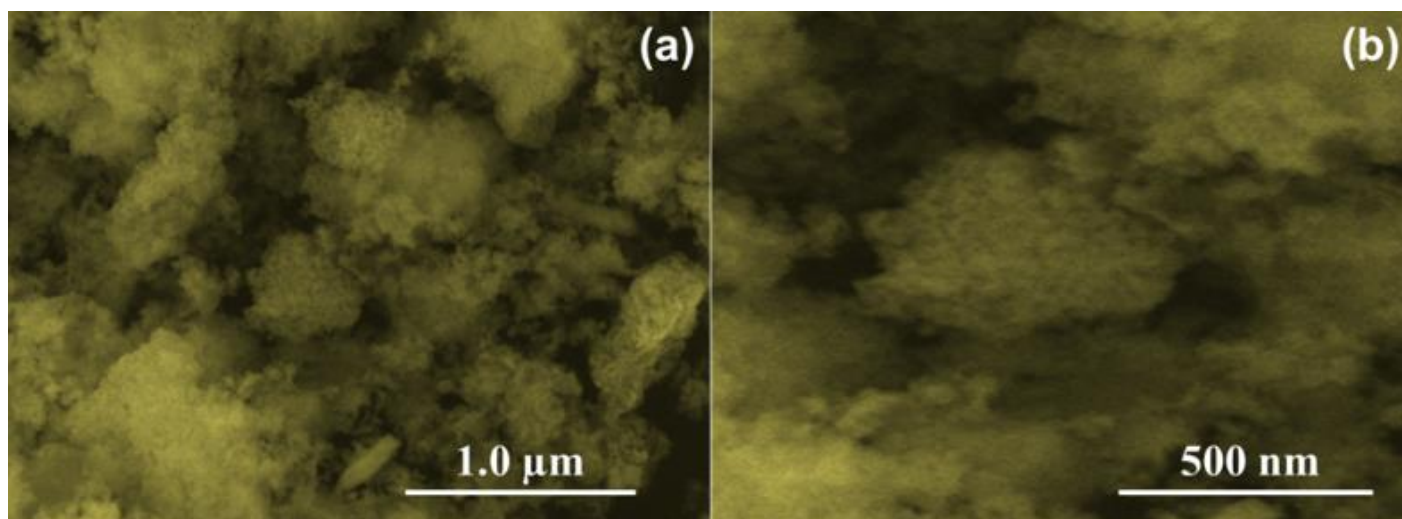

Fig. 1. Suggested steps for synthesis of FeLO NPs.

Fig. 2. XRD pattern of the FeLO NPs.

Fig. 3. (a) Low, and (b) high-magnification SEM images of the FeLO NPs.

Fourier-transform infrared spectroscopy analysis of FeLO nanoparticles displayed prominent peaks at 3430, 1469, 1028, and 574.5 cm^{-1}. The peak at 3430 cm^{-1} is characteristic of -OH stretching vibrations (Figure 4). The sharp peak at 574.5 cm^{-1} suggests the stretching vibrations of the Fe-O bond. Notably, additional peaks at 594.5 and 461.5 cm^{-1} were observed, likely representing Fe-O and La-O bond vibrations, respectively [12-16]. These findings confirm the presence of specific functional groups and bonding interactions within the nanoparticle structure, indicative of their complex molecular composition.
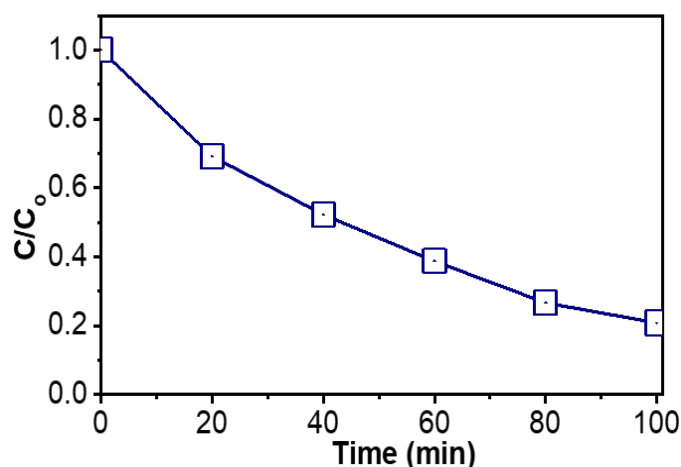
The surface area of the FeLO nanoparticles, as measured by the Brunauer-Emmett-Teller (BET) method, was determined to be 2.43 square meters per gram. This measurement indicates the extent of the surface available for interactions or reactions (Figure 5).
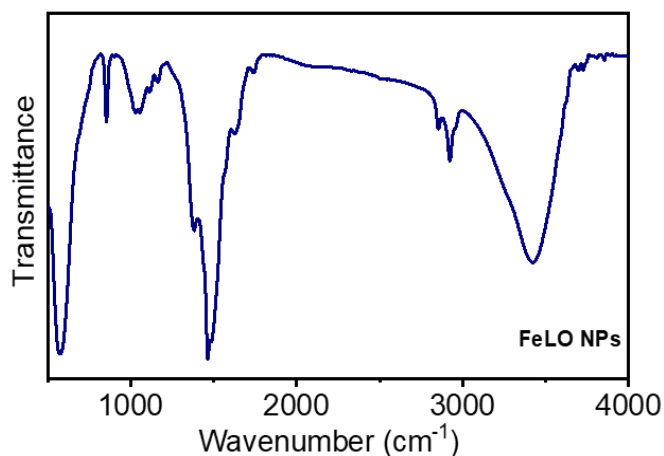
Fig. 4. FTIR spectrum of the FeLO NPs.
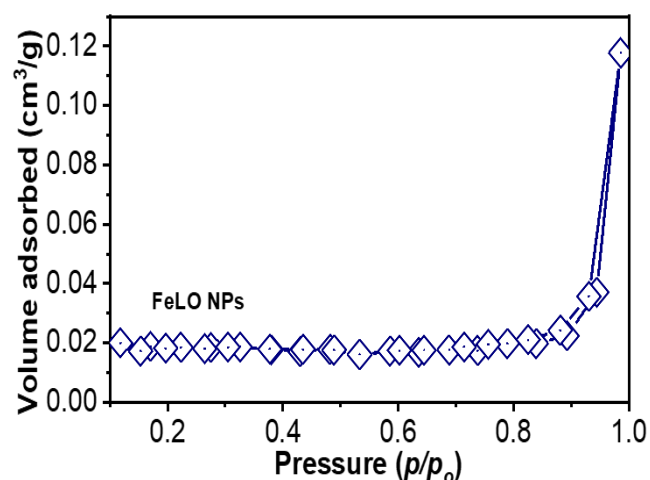
Fig. 5. N$_2$ adsorption-desorption profile of the FeLO NPs.

Fig. 6. C/C$_0$ degradation of MB degradation for the FeLO NPs photocatalyst.

The photocatalytic performance of the FeLo nanoparticles was evaluated through the degradation of the model organic dye methylene blue (MB), commonly used in textile industries (Figure 6). This assessment was conducted under conditions of visible light exposure. The results, illustrated in the corresponding figure, demonstrate that the FeLO nanoparticles possess significant photocatalytic degradation capabilities (Figure 6).

Notably, they achieved approximately 90% degradation of the dye, displaying their effectiveness in breaking down MB when exposed to visible light. This highlights the potential of FeLo NPs for environmental remediation applications, particularly in treating dye-polluted wastewater.

The photocatalytic performance of the FeLo nanoparticles was evaluated through the degradation of the model organic dye methylene blue (MB), commonly used in textile industries (Figure 6). This assessment was conducted under conditions of visible light exposure. The results, illustrated in the corresponding figure, demonstrate that the FeLO nanoparticles possess significant photocatalytic degradation capabilities (Figure 6).

Notably, they achieved approximately 90% degradation of the dye, displaying their effectiveness in breaking down MB when exposed to visible light. This highlights the potential of FeLo NPs for environmental remediation applications, particularly in treating dye-polluted wastewater.

In the study depicted in the figure, the degradation pathway of MB via FeLO nanoparticles under UV irradiation is elucidated (Figure 7). During this process, photons activate the catalyst, resulting in the separation of electron-hole pairs [5-13]. Holes in the valence band interact with water molecules or hydroxide ions on the surface to form hydroxyl radicals. Simultaneously, electrons are promoted to the conduction band of FeLO nanoparticles, enhancing the separation and migration of photogenerated charge carriers [1-9]. These electrons then combine with oxygen molecules to create superoxide radicals. Both hydroxyl and superoxide radicals, once formed, detach from the surface of the catalysts and engage the pollutants, effectively breaking them down. This mechanism underlines the role of radical species in the photocatalytic degradation of contaminants.
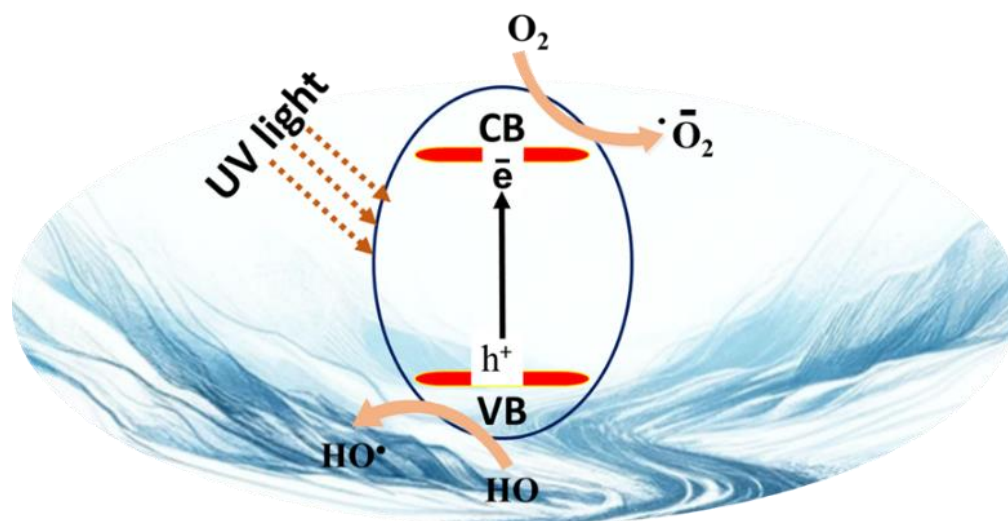
Fig. 7. Proposed mechanism of MB degradation at the FeLO NPs photocatalyst surface.

4. CONCLUSIONS

The research conducted on iron lanthanum oxide nanoparticles (FeLO NPs) demonstrates their robust capabilities in photocatalytic applications, particularly for the degradation of organic pollutants in water. The synthesis of FeLO NPs through a co-precipitation method proved effective, yielding nanoparticles with desirable crystalline structures and heterogeneous surface morphologies, as confirmed by X-ray diffraction and scanning electron microscopy. The specific surface area measured at 2.43 m²/g facilitates extensive surface interactions crucial for photocatalytic activities. Fourier-transform infrared spectroscopy highlighted the presence of functional groups essential for the stability and activity of the nanoparticles. Photocatalytic experiments revealed that FeLO NPs exhibit high efficiency in degrading methylene blue, achieving up to 90% reduction under controlled light conditions. This significant degradation capacity is attributed to the effective generation of reactive radical species, initiated by the excitation of electrons and facilitated by the unique electronic properties of the nanoparticles. The stability and reusability of FeLO NPs further enhance their practical utility in environmental remediation. These findings suggest that FeLO nanoparticles hold substantial promise as a sustainable solution for purifying dye-polluted wastewater, showcasing their potential in broader environmental cleanup efforts.

CONFLICT OF INTEREST

The authors declare that there is no conflict of interests.

ACKNOWLEDGEMENTS

REFERENCES

[1] Khammarnia, S., Akbari, A., Saffari, J. and Ekrami-Kakhki, M.S., **2019.** Synthesis of FeLaO₃ and FeNdO₃ Magnetic Nanocomposites as Photocatalyst for Organic Dye Removal. *Journal of Cluster Science*, *30*(6), pp.1383-1391.

[2] Babu, C.M., Palanisamy, B., Sundaravel, B., Shanthi, K. and Murugesan, V., **2015.** Dihalogen crosslinked Fe₃O₄-reduced graphene oxide nanocomposites for arsenic and mercury adsorption. *Science of Advanced Materials*, *7*(4), pp.794-805.

[3] Chen, M., Chen, Z., Wu, P. and Chen, J.P., **2021.** Simultaneous oxidation and removal of arsenite by Fe (III)/CaO₂ Fenton-like technology. *Water Research*, *201*, p.117312.

[4] Dinda, D. and Saha, S.K., **2015.** Sulfuric acid doped poly diaminopyridine/graphene composite to remove high concentration of toxic Cr (VI). *Journal of Hazardous Materials*, *291*, pp.93-101.

[5] Han, C., Zhang, L., Chen, H., Shan, X., Li, X., Zhu, W. and Luo, Y., **2016.** Removal As (V) by sulfated mesoporous Fe–Al bimetallic adsorbent: Adsorption performance and uptake mechanism. *Journal of Environmental Chemical Engineering*, *4*(1), pp.711-718.

[6] Jais, F.M., Ibrahim, S., Yoon, Y. and Jang, M., **2016.** Enhanced arsenate removal by lanthanum and nano–magnetite composite incorporated palm shell waste–based activated carbon. *Separation and Purification Technology*, *169*, pp.93-102.

[7] Jiang, B., Li, L., Zhang, Q., Ma, J., Zhang, H., Yu, K., Bian, Z., Zhang, X., Ma, X. and Tang, D., **2021.** Iron–oxygen covalency in perovskites to dominate syngas yield in chemical looping partial oxidation. *Journal of Materials Chemistry A*, *9*(22), pp.13008-13018.

[8] Kang, J.G., Kim, Y.I., Cho, D.W. and Sohn, Y., **2015.** Synthesis and physicochemical properties of La (OH) 3 and La₂O₃ nanostructures. *Materials Science in Semiconductor Processing*, *40*, pp.737-743.

[9] Kobyliukh, A., Olszowska, K., Godzierz, M., Kordyka, A., Kubacki, J., Mamunya, Y., Pusz, S., Stoycheva, I. and Szeluga, U., **2022.** Effect of graphene material structure and iron oxides deposition method on morphology and properties of graphene/iron oxide hybrids. *Applied Surface Science*, *573*, p.151567.

[10] Zhou, X., Vovk, E.I., Liu, Y., Guan, C. and Yang, Y., **2021.** An in situ temperature-dependent study of La₂O₃ reactivation process. *Frontiers in Chemistry*, *9*, p.694559.

[11] Katba, S., Jethva, S., Vagadia, M., Ravalia, A. and Kuberkar, D.G., **2020.** Effect of La-substitution on magnetic properties of ErFeO₃ orthoferrites. *Journal of Magnetism and Magnetic Materials*, *514*, p.167170.

[12] Oliveira, A., Hneda, M.L., Fernandez-Outon, L.E., de Sousa, E.M.B. and Ardisson, J.D., **2019.** Synthesis and characterization of nanocomposites based on rare-earth orthoferrites and iron oxides for magnetic hyperthermia applications. *Ceramics International*, *45*(14), pp.17920-17929.

[13] Jadhav, A.D., Gaikwad, A.B., Samuel, V. and Ravi, V., **2007.** A low temperature route to prepare LaFeO₃ and LaCoO₃. *Materials Letters*, *61*(10), pp.2030-2032.

[14] Vázquez-Vázquez, C., Kögerler, P., Lopez-Quintela, M.A., Sánchez, R.D. and Rivas, J., **1998.** Preparation of LaFeO₃ particles by sol-gel technology. *Journal of materials research*, *13*(2), pp.451-456.

[15] Pecchi, G., Reyes, P., Zamora, R., Campos, C., Cadús, L.E. and Barbero, B.P., **2008.** Effect of the preparation method on the catalytic activity of La₁₋ₓCaₓFeO₃ perovskite-type oxides. *Catalysis Today*, *133*, pp.420-427.

[16] Tong, F., Zhao, Y. and Wang, M.H., **2019.** Cube-like LaFeO₃ microstructures synthesised by a hydrothermal method and their optical properties. *Micro & Nano Letters*, *14*(3), pp.259-262.